Conformational Processes in L-Alanine Studied Using Dual Space Analysis

Chantal T. Falzon and Feng Wang

Centre for Molecular Simulation, Swinburne University of Technology, P.O. Box 218, Hawthorn, Melbourne, Victoria, Australia, 3122
fwang@swin.edu.au

Abstract. Binding energy spectra and orbital momentum distributions of the two most stable conformers of L-alanine are investigated. Molecular properties such as geometry and dipole moments agree well with available experimental and previous theoretical investigations. Dual space analysis is employed to study the binding energy spectra in coordinate space based on B3LYP/TZVP density functional calculations, and the valence orbital momentum distributions based on the plane wave impulse approximation. In the valence space, the HOMO (24*a*), NHOMO (23*a*) and orbitals 22*a* and 18*a* are selected to study the conformational processes in L-alanine.

1 Introduction

The behaviour of proteins in biological systems at the molecular level is an important area of research, since many biological phenomena can be traced to fundamental properties of the molecular constituents. The native structures of proteins are largely governed by the balance of interactions among the different amino acid residues. Understanding the biological specificity of these species therefore requires insight into the dynamics of amino acids (NH_2-CH(R)-COOH). The functionality of amino acids varies depending on their conformation [1], which is important in protein stability and three dimensional folding [2]. Therefore, analysis of structural and chemical properties of amino acids under isolated conditions is of great importance.

Alanine (R=CH_3) is an important prototype for all chiral amino acids, due to its relatively simple structure. In the body, it has a major role in transferring nitrogen from tissue sites to the liver [3]. The conformational behaviour of L-alanine, like glycine [4], has brought many challenges to experimental and theoretical investigations. Up to 13 conformations were predicted from sophisticated *ab initio* calculations [5, 6], several of which were observed experimentally using the millimetre wave (MMW) spectrum of alanine [7] and gas-phase electron diffraction (GED) techniques [8]. The relative stability of these conformers is dependant upon the interplay of various intramolecular hydrogen bonds and electron correlation, as demonstrated for small aliphatic amino acids [4, 6, 9].

In position space, the conformational processes of L-alanine has been investigated, using both DFT and *ab initio* methods [6]. Molecular properties, such as geometries, relative energies and dipole moments have all been effectively predicted using similar

V.N. Alexandrov et al. (Eds.): ICCS 2006, Part III, LNCS 3993, pp. 82 – 88, 2006.

models [5, 6]. The two lowest energy conformations for L-alanine, **I** and **II**, are presented in Fig. 1. Details however regarding the redistribution of electron density and orbital distortion, as a result of these processes, are lacking. This study therefore aims to provide an orbital-based insight into the bonding environment within L-alanine. We focus on information that differentiates the conformers, such as dipole moments and orbital momentum distributions (MDs), using dual space analysis (DSA) [10]. Conformational variations will be discussed in relation to rotations about the $C_{(3)}$-O, $C_{(3)}$-C_α and C_α-N bonds, in order to provide an orbital dependant representation of the bonding mechanisms within the two conformations.

2 Methods and Computational Details

Density functional theory (DFT) B3LYP methodology, together with the triple zeta valence polarized (TZVP) basis set [11] was employed for geometry optimization calculations. Electronic structural calculations undertaken in this study used the computational chemistry package of GAUSSIAN03 [12].

Molecular wave functions obtained from single point calculations (B3LYP/TZVP//B3LYP/TZVP) were Fourier transformed into **k**-space as momentum distributions (MDs, σ). Under the Born-Oppenheimer approximation, independent particle approximation and the plane wave impulse approximation (PWIA) [13] gives,

$$\sigma \propto \int d\mathbf{\Omega} \mid \psi_j(\mathbf{k}) \mid^2 \tag{1}$$

The integral $d\mathbf{\Omega}$ performs the spherical averaging over the initial rotational states, while σ is proportional to the squared momentum space one-electron Dyson orbitals $\psi_j(\mathbf{k})$. The azimuthal angle ϕ has a defined relationship with momentum [13].

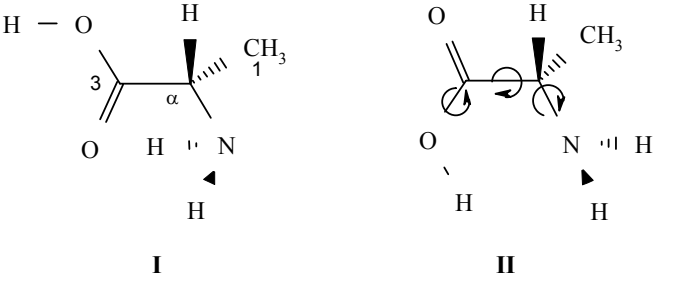

Fig. 1. Chemical structures and numbering system of the L-alanine conformers calculated using the DFT-B3LYP/TZVP model

3 Results and Discussion

3.1 Geometric Correlation of the L-Alanine Conformers

Conformer **I** is the most abundant conformation [1, 7] and represents the global minimum structure on the torsional potential surface. Conformer **II**, the second most

populated conformation (~8:1 ratio in favour of **I**) is produced by three rotations of the $C_{(3)}$-C_α, $C_{(3)}$-O and C_α-N bonds in conformer **I**. Selected geometric parameters for these conformations based on the B3LYP/TZVP model are given in Table 1.

The predicted properties for both conformations agree well with previous experimental and theoretical results. All bond lengths lie within 0.02Å of the experiment, whilst most angular deviations were less than 3°. The exception however is in the description of the ∠HOC angle in **I**. The B3LYP/TZVP model predicted this angle to be 107°, which is 5.3° smaller than the experimental value of 112.3°. A similar deviation was observed by Császár [6] (decrease of 6.1°) when using the MP2/6-311++G** method.

Table 1. Optimized geometrical parameters for conformers **I** and **II** of L-alanine obtained using the B3LYP/TZVP model. Experimental and previous theoretical calculations are provided for comparison.

Paramters	**Expt**[a]		**B3LYP**	**/TZVP**	**MP2**	**/6-311++G****[b]
	I	**II**	**I**	**II**	**I**	**II**
$C_{(3)}$-C_α/Å	1.527	1.538	1.528	1.542	1.521	1.533
C_α-$C_{(1)}$/Å	1.536	1.532	1.537	1.532	1.530	1.527
$C_{(3)}$-O/Å	1.341	1.327	1.360	1.344	1.356	1.342
C_α-N/Å	1.453	1.469	1.457	1.477	1.452	1.468
O-HÅ	0.977	—	0.972	0.987	0.968	0.980
O=$C_{(3)}$-C_α/°	125.6	122.9	125.6	122.8	125.4	122.6
$C_{(3)}$-C_α-N/°	112.9	108.6	113.5	109.5	113.7	109.4
H-O-$C_{(3)}$/ °	112.3	—	107.0	104.9	106.2	104.0
O=$C_{(3)}$-C_α-$C_{(1)}$/°		—	-75.5	-101.8	-76.6	-101.7
O=$C_{(3)}$-C_α-N/°	-16.6	—	-19.7	-168.4	-20.5	-164.4
H-O-$C_{(3)}$-C_α/ °	180.0	—	178.2	-2.7	176.9	-5.4
Dipole Moment[c]						
μ_x/D	0.62	4.92	0.71	-5.43	0.64	5.24
μ_y/D	1.60	1.40	0.99	-1.38	1.19	1.44
μ_z/D	0.34	0.28	-0.46	-0.65	0.42	0.40
μ/D	1.80	5.13	1.31	5.64	1.41	5.45
ΔE/kcal·mol^{-1}			0.0	-0.014	0.0	0.14 (0.03)[d]
ΔE_{ZPE}/kcal·mol^{-1}			0.0	0.20	0.0	0.39[e]

[a]Electron diffraction, Ref [8].
[b]geometry, see Ref [6]; Dipole moment see Ref [1].
[c] Experimental data based on Millimetre-Wave Spectroscopy, Ref [9].
[d]B3LYP/6-311++G**, Ref [6].
[e]B3LYP/aug-cc-pVDZ, Ref [14]

In table 1, rotations around the single bonds do not exhibit impact on bond lengths; small angle variations are however observed and apparent changes in dihedral angles exist to accommodate the rotations. This is highlighted by the elongation of the C_{α}-N bond (0.02Å) and the reduction in the $\angle C_{(3)}C_{\alpha}N$ angle (4°) in **II**, resulting from the weak OH···NH_2 interaction (H···N distance is 1.899 Å). The results obtained in this study agree well with both experimental and previous theoretical calculations.

3.2 Conformational Impact on Stability and Molecular Properties

A number of important molecular properties using DFT [6, 14] and *ab initio* calculations [1, 6] are provided in Table 1 for comparison. With the inclusion of zero-point energy (ZPE), the present method predicts conformer **II** to lie within 0.20 kcal·mol^{-1} of **I**. This is in satisfactory agreement with the values of 0.14 and 0.39 kcal·mol^{-1} given by the MP2/6-311++G** and B3LYP/aug-cc-pVDZ [14] (ZPE included) models, respectively.

Properties such as dipole moments are also included in this table as biomolecular conformers that differ by small energies can exhibit profound differences in their anisotropic properties [4], affecting their chemical reactivity. The $C_{(3)}$-C_{α}, C_{α}-N and $C_{(3)}$-O bond rotations in **I** cause the total dipole moment to increase significantly from 1.31 D to 5.64 D, which agrees well with the experimental values of 1.80 D (**I**) and 5.13 D (**II**) [9] and the values of 1.41 D and 5.45 D generated using the MP2/6-311++G** model [1]. Such changes indicate that significant charge redistribution is associated with these rotations. This is also evident as μ_x and μ_y have altered considerably as a result of these rotations. For example, μ_x of **I** is 0.72 D and becomes -5.43 D in conformer **II**, whilst μ_z varies significantly without any changes in sign. This trend was observed in glycine [4].

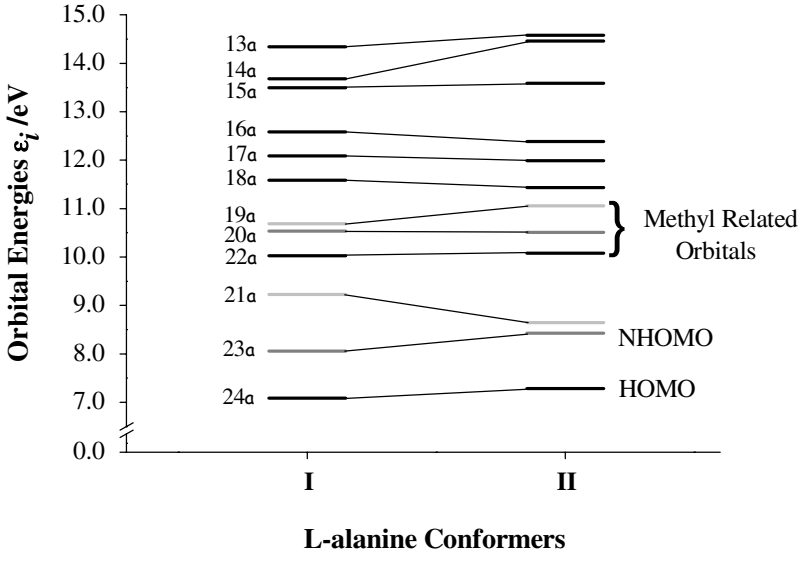

Fig. 2. Outer valence orbital energies for the L-alanine conformer calculated using the B3LYP/TZVP model

3.3 Molecular Orbital Information in Coordinate Space

In their ground electronic states, conformers **I** and **II** (X1*A*) of L-alanine are both closed shells with singlet states, which have 24 doubly occupied molecular orbitals (MOs). The associated orbital energies for these conformations are given in Fig. 2. From this figure it is clear the three combined bond rotations in **I** cause major energy variations in orbitals 14*a*, 19*a*, 22*a* and 23*a*, whilst visible changes to orbitals 13*a*, 16*a*, 18*a* and 24*a* are observed. From information provided thus far it is still unclear as to the changes in the nature of bonding from these rotations. This will be explored in more detail in the next sections using information from momentum space.

3.4 Orbital MDs of L-Alanine in Valence Space

Orbital momentum distributions (MDs) of L-alanine in the outer valence space have been calculated in the present study. Both conformations belong to the C_1 point group symmetry and their Dyson orbitals are therefore correlated. Four representative orbitals were selected to demonstrate interesting structural information of L-alanine (Fig. 3). Orbitals of other conformers which exhibit the most significant variation with respect to the global minimum structure of L-alanine are considered to be the fingerprints of rotation around a particular bond.

In Figure 3(a), orbital MDs related to MO 24a (HOMO) indicate significant mixed 's-like' and '*p*-like' characteristics in both conformations. The associated charge distributions of the Dyson orbital reveal that in **I** these contributions are predominately from the lone-pair on the N atom and N-H bonds of the amino group. The rotations enhance contributions on the lone-pair of the O in $O{=}C_{(3)}$, whilst reducing the charge density on the amino group. The latter reduces the orbital density of H atoms in the $-NH_2$ group, causing the momentum distributions to drop in the low momentum region. This may have significant implications in the chemical reactivity of these conformers as any structural manipulation, i.e., bond breaking or bond formation occurs within these frontier orbitals.

In MO 23*a* (NHOMO), the nature of bonding in the two conformations are essentially reversed. That is, the *p*-like contributions in **I** are primarily from the lone pair on O of $O{=}C_{(3)}$, whereas in conformer **II** the contributions stem from the amino group [Fig. 3(b)]. Sizeable *s*-contributions are also present along the C_α-N bond, contributing to the enhancement of the orbital MDs in the region of low momentum. This demonstrates that orbital MDs can serve as a quantitative property in the identification of electron redistribution. Similar trends to the HOMOs and NHOMOs were observed in the glycine conformers [4], where rotation of the $C_{(3)}$-C_α and C_α-N bonds were shown to cause the most perturbation to the orbitals in this region.

In contrast, MO 22*a* in Fig. 3(c) demonstrates that the electron charge distributions concentrating in the HO-C=O region in **I** did not change with the single bond rotations, even with the rotation of the HO-C bond. A small enhancement of charge density on the NH_2 group in **II** causes the small shift of orbital MDs towards the low momentum region, as indicated in Fig 3(c). In both conformations, this MO is clearly a π-bond with the nodal plane being the molecular plane, which is formed by the non-hydrogen atoms (excluding the methyl group). These orbitals are related to the anti-symmetric orbitals of *a*'' symmetry found in glycine [4, 15].

In comparison to MOs 24*a* and 23*a* (Fig 3 (a) and (b)), where the discrepancies in the momentum distributions occur at zero momentum due to the hydrogen 1s AO contributions, orbital 18*a* in **I** and **II** differ in the region of medium momentum at approximately $\phi = 10°$ (Fig. 3(d)). This orbital correlates to orbital 14*a*' in glycine [4], which was shown to be the fingerprint orbital for all single bond rotations. In MO 18*a*, rotation of $C_{(3)}$-O in **I** caused the strong delocalised coverage along the H-O-$C_{(3)}$-C_α framework to break into more isolated groups of H-O-$C_{(3)}$, $C_{(3)}$=O and $C_{(3)}$-C_α-$C_{(1)}$. These changes are reflected in the associated orbital MDs in Fig. 3(d).

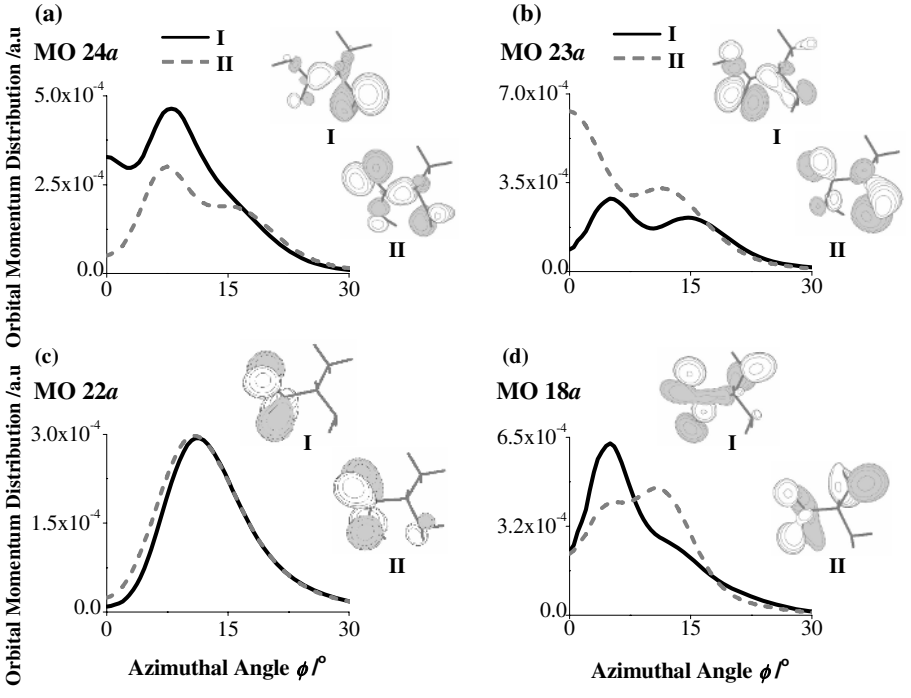

Fig. 3. Momentum distributions and charge distributions of selected orbitals (24*a*, 23*a*, 22*a* and 18*a*) for conformers **I** and **II**. Dyson orbitals are plotted using Molden [16].

4 Conclusion

Rotational processes of the two lowest energy conformers of L-alanine (X*A*) have been studied using dual space analysis (DSA). Changes to the geometric parameters after the $C_{(3)}$-C_α, C_α-N and $C_{(3)}$-O bond rotations in the global minimum (**I**) largely resulted from the related dihedral angles reflecting the rotations. Weak interactions, such as O-H···NH_2 also contribute to the changes in structure. Between the two conformations, redistribution of the electron charge density was also found to vary significantly in certain orbitals.

Variations in both binding energy spectra and orbital momentum distributions in L-alanine were observed as a result of the rotations. Orbitals exhibiting significant changes in binding energy however did not necessarily vary significantly in the shape of their electron density (orbital MDs) and vice versa. While the HOMO (24*a*) and orbital 18*a* did not exhibit major changes in their binding energies with respect to their conformations, however these orbitals experienced significant variations in their electron density, as reflected by their orbital MDs. Orbital 22*a* receives significant changes in binding energy but its electron density does not vary much with respect to conformation. Using dual space analysis, this investigation therefore provides a unique insight into the structural effects of alanine upon rotation.

Acknowledgements. The authors thank the Vice-Chancellor's Strategic Research Initiative Grant of Swinburne University of Technology and the Australian Partnership for Advanced Computing for the use of the National Supercomputing Facilities.

References

1. Blanco, S *et al*., *J. Am. Chem. Soc*., **126**, (2004), 11675.
2. Baldwin, T.; Lapointe, M in *The Chemistry of Amino Acids. The Biology Project [Online]*, http://www.biology.arizona.edu/biochemistry/problem_sets/aa/aa.html, 2003.
3. Rennie, M. J. in *Physical Exertion, Amino Acid and Protein Metabolism and Protein Requirements; Proteins and Amino Acids.* Washington, DC: National Academy Press, (1999).
4. Falzon, C. T., Wang, F. *J. Chem. Phys*., **123,** (2005), 214307.
5. (a) Cao, M., *et al*., *J. Mol. Struct*: *THEOCHEM*, **332**, (1995), 251. (b) Godfrey, P. D., *et al*., *J. Mol. Struct*., **376**, (1996), 65. (c) Kaschner, R., Hohl, D. *J. Phys. Chem. A*., **102**, (1998), 5111.
6. Császár, A. G. *J. Phys. Chem*., **100**, (1996), 3541.
7. Godfrey, P. D., *et al*., *J. Am. Chem. Soc*., **115**, (1993), 9687.
8. (a) Iijima, K., Beagley, B. *J. Mol. Struct*., **248**, (1991), 133. (b) Iijima, K., Nakano, M. *J. Mol. Struct*., **485-486**, (1999), 255.
9. Lesarri, A. *et al*., *Angew. Chem. Int. Ed*., **43**, (2004), 605.
10. Wang, F. *J. Phys. Chem. A*., **107**, (2003), 10199.
11. Godbout, N., *et al*., *Can. J. Chem*., **70**, (1992), 560.
12. Frisch, M. J., *et al*., *Gaussian Inc*; Wallingford: CT, (2004).
13. McCarthy, I. E., Weigold, E. *Rep. Prog. Phys*. **54**, (1991), 789.
14. Stepanian, S. G., *et al*., *J. Phys. Chem. A*., **107**, (1998), 4623.
15. Falzon, C. T., Wang, F., Pang, W. N., J. Phys. Chem. B., 000, (2006), 0000.
16. Schaftenaar, G., Noordik, J. *J. Comput-Aided Mol. Design.,* **14**, (2000), 123.